ARTICLE

Bidirectional ephrinB2-EphB4 signaling controls bone homeostasis

Chen Zhao,[1,5] Naoko Irie,[1,5] Yasunari Takada,[1] Kouji Shimoda,[2] Takeshi Miyamoto,[3] Toru Nishiwaki,[4] Toshio Suda,[3] and Koichi Matsuo[1,*]

[1] Department of Microbiology and Immunology
[2] Laboratory Animal Center
[3] The Sakaguchi Laboratory of Developmental Biology
[4] Department of Orthopedic Surgery
School of Medicine, Keio University, Shinjuku-ku, Tokyo, 160-8582, Japan
[5] These authors contributed equally to this work.
*Correspondence: matsuo@sc.itc.keio.ac.jp

Summary

Bone homeostasis requires a delicate balance between the activities of bone-resorbing osteoclasts and bone-forming osteoblasts. Various molecules coordinate osteoclast function with that of osteoblasts; however, molecules that mediate osteoclast-osteoblast interactions by simultaneous signal transduction in both cell types have not yet been identified. Here we show that osteoclasts express the NFATc1 target gene *Efnb2* (encoding ephrinB2), while osteoblasts express the receptor EphB4, along with other ephrin-Eph family members. Using gain- and loss-of-function experiments, we demonstrate that reverse signaling through ephrinB2 into osteoclast precursors suppresses osteoclast differentiation by inhibiting the osteoclastogenic c-Fos-NFATc1 cascade. In addition, forward signaling through EphB4 into osteoblasts enhances osteogenic differentiation, and overexpression of EphB4 in osteoblasts increases bone mass in transgenic mice. These data demonstrate that ephrin-Eph bidirectional signaling links two major molecular mechanisms for cell differentiation—one in osteoclasts and the other in osteoblasts—thereby maintaining bone homeostasis.

Introduction

Bone-resorbing osteoclasts are large, multinucleated cells derived from monocyte-macrophage precursors, while bone-forming osteoblasts are derived from mesenchymal cells (Karsenty and Wagner, 2002; Teitelbaum and Ross, 2003). Osteoblasts or bone stromal cells produce macrophage-colony stimulating factor (M-CSF, encoded by *Csf1*) and RANK ligand (RANKL). When these cytokines stimulate their receptors on osteoclast precursors, downstream signaling pathways activate the transcription factors NF-κB (Franzoso et al., 1997), c-Fos (Grigoriadis et al., 1994), and NFATc1 (nuclear factor of activated T cells c1) (Asagiri et al., 2005; Ishida et al., 2002; Takayanagi et al., 2002a), all of which are required for osteoclast differentiation. Mice lacking c-Fos ($Fos^{-/-}$ mice) develop osteopetrosis due to an osteoclast differentiation block. We reported that *Nfatc1* is a major c-Fos target gene and that a constitutively active form of NFAT restores the differentiation block in $Fos^{-/-}$ osteoclast precursors (Matsuo et al., 2004). In addition, c-Fos activates transcription of *Ifnβ* (encoding IFN-β), which mediates a negative feedback loop that suppresses osteoclast differentiation (Takayanagi et al., 2002b).

Bone remodeling is a complex process requiring "coupling" between osteoclastic and osteoblastic activities. Coordinated function of osteoclasts and osteoblasts ensures that resorption lacunae are filled with new bone produced by osteoblasts so as to maintain bone integrity. Mechanical forces and certain systemic factors, such as steroids or parathyroid hormone, affect bone remodeling. For the anabolic effect of parathyroid hormone to occur, bone resorption may be necessary, implying that osteoblast formation requires signals from osteoclasts (Martin, 2004). Local factors including TRAP secreted by osteoclasts (Sheu et al., 2003) and insulin-like growth factor and transforming growth factor-β, which are released from bone matrix during bone resorption (Hayden et al., 1995; Pfeilschifter and Mundy, 1987), can stimulate bone formation. An imbalance between bone resorption and formation results in bone remodeling diseases such as osteoporosis and osteopetrosis. Even auditory ossicles, the smallest bones in the body, can be adversely affected by defects in bone remodeling (Kanzaki et al., 2006). Understanding the mechanisms underlying bone remodeling should potentially facilitate prevention and treatment of bone remodeling diseases.

Cell-surface molecules ephrinB (B1∼B3) are preferential ligands for the tyrosine kinase receptors EphB (B1∼B6), while ephrinA proteins (A1∼A5) function as ligands for EphA (A1∼A10) receptors (Himanen and Nikolov, 2003; Kullander and Klein, 2002; Murai and Pasquale, 2003; Palmer and Klein, 2003; Pasquale, 2005). The ephrinB family consists of transmembrane proteins with cytoplasmic domains, whereas the ephrinA family consists of glycosyl-phosphatidyl inositol (GPI)-anchored molecules. Interaction between ephrinB- and EphB-expressing cells results in bidirectional signal transduction. Activation of the EphB receptors by the ephrinB ligands is referred to as "forward signalling," whereas activation of the ephrinB ligands by the EphB receptors is designated "reverse signalling." Reverse signaling through ephrinB ligands activates both tyrosine phosphorylation-dependent and -independent signal transduction pathways. The intracellular domain of ephrinB ligands, particularly the last 33 C-terminal amino acids, is

highly conserved and contains multiple tyrosine residues, and the C-terminal YKV motif is a binding site for PDZ (postsynaptic density protein, disks large, zona occludens) domain-containing proteins. Similarly, forward signaling through EphB receptors activates both tyrosine phosphorylation-dependent and -independent pathways. The importance of bidirectional signaling has been confirmed in angiogenesis, axon guidance, cell sorting, and boundary formation (Davy and Soriano, 2005). For example, ephrinB2 and its cognate receptor EphB4 are reciprocally expressed in arterial and venous endothelial cells. Mice deficient in ephrinB2 or EphB4 exhibit similar phenotypes characterized by early embryonic lethality due to disorganized arteriovenous formation (Adams et al., 1999; Gerety et al., 1999; Wang et al., 1998). However, recent analysis using ephrinB2 mutants lacking the C-terminal cytoplasmic domain revealed that ephrinB2 reverse signaling through the cytoplasmic domain is not required for early vascular development but is required for axon pathfinding and cardiac valve formation (Cowan et al., 2004). Furthermore, ephrin-Eph interaction regulates stem cell differentiation (Wang et al., 2004), the immune response (Sharfe et al., 2002; Yu et al., 2003), intestinal epithelial cell migration (Batlle et al., 2002), and skeletal patterning (Compagni et al., 2003; Davy et al., 2004).

Here we identify *Efnb2* (encoding ephrinB2) as an NFAT target gene during osteoclast differentiation. In addition we show that EphB4 is expressed on osteoblasts. Using a combination of in vitro and in vivo approaches we demonstrate that ephrinB2-EphB4 bidirectional signaling links suppression of osteoclast differentiation to stimulation of bone formation, which may regulate the transition from a bone-resorption to a bone-formation phase in each bone remodeling cycle.

Results

Expression of ephrinB and EphB families in bone cells

Overexpression of an active form of NFAT in $Fos^{-/-}$ osteoclast precursors induces expression of *Efnb2* in addition to upregulation of osteoclast markers such as *Acp5* (encoding tartrate-resistant acid phosphatase, TRAP) and *Calcr* (encoding the calcitonin receptor) (Matsuo et al., 2004). Therefore, we examined *Efnb2* expression by quantitative reverse transcription-polymerase chain reaction (RT-PCR) analysis using M-CSF-dependent macrophages (MDMs) derived from bone marrow or spleen cells as osteolast precursors. Expression of the macrophage marker *Fcgr3* (CD16) was higher in $Fos^{-/-}$ cultures than in wild-type cultures (Figure 1A). Interestingly, expression of *Efnb2* was induced in the presence of RANKL for 3 days along with *Acp5* and *Calcr* in wild-type but not in $Fos^{-/-}$ cultures by RANKL (Figure 1A). Next we identified an NFAT binding site (−2863 relative to the ATG initiation codon) in the mouse *Efnb2* promoter by electrophoretic mobility shift assays (EMSA) and showed that an *Efnb2* promoter-reporter construct is activated by RANKL or NFAT (Figure S1). At the protein level, ephrinB2 was induced during osteoclast differentiation (Figure 1B). Using immunofluorescence microscopy, we detected ephrinB2 protein in multinucleated and differentiating mononuclear osteoclasts formed in the presence of RANKL and intact *Fos* (Figure 1C, Wt). When cells were immunostained before fixation and permeabilization, ephrinB2 was detected on the membrane of wild-type osteoclasts (Figure 1C, membrane). Finally, we detected ephrinB2 expression in TRAP-positive multinucleated osteoclasts in bone sections (Figure 1D). These data demonstrate that *Efnb2* expression is induced during osteoclast differentiation through the c-Fos-NFATc1 transcriptional cascade in wild-type cells.

Because ephrinB2 is known to interact with the receptors EphB1, EphB2, EphB3, EphB4, EphB6, and EphA4, we examined expression of *Efnb* and *Ephb* family members and *Epha4* in osteoclasts and osteoblasts differentiated in vitro. In differentiating osteoclasts, mRNAs of *Efnb1* and *Efnb2* encoding ligands but not *Ephb* encoding receptors were detected (Figure 1E). By contrast, calvarial osteoblasts constitutively expressed several *Efnb* ligands, *Ephb* receptors, and *Epha4* (Figure 1E).

Reverse signaling suppresses osteoclast formation

The indiscriminate ephrinB2 interacts with multiple Ephs, while EphB4 only interacts with ephrinB2 (Gale and Yancopoulos, 1999; Myshkin and Wang, 2003). Therefore, to analyze the effects of reverse signaling in osteoclast differentiation we used EphB4 to stimulate ephrinB2, and to analyze the effects of forward signaling in osteoblast differentiation we used ephrinB2 to stimulate Eph receptors. Addition of clustered EphB4 to osteoclastogenic cultures suppressed osteoclast differentiation and hence bone resorption in a dose-dependent manner (Figure 2A). To investigate whether membrane bound EphB4 also suppresses osteoclast differentiation through ephrinB2, we established subclones of ST2 stromal cells stably expressing EphB4. Quantitative RT-PCR analysis showed that forced expression of EphB4 did not reduce RANKL or M-CSF or increase osteoprotegerin (OPG) expression levels (Figure S2). We then cocultured bone marrow cells with EphB4-expressing ST2 cells. Consistent with the soluble EphB4 experiment, membrane bound EphB4 also suppressed osteoclast formation (Figure 2B). In addition to soluble EphB4, we treated osteoclast precursors with soluble EphA4 and EphB2, which are known to interact with ephrinB2. As a negative control, we used ephrinB2 itself since ephrinB2 does not interact homophilically. The soluble receptors EphB4, EphA4, and EphB2 but not the soluble ligand ephrinB2 suppressed osteoclastogenesis as evidenced by *Calcr* expression (Figure 2C). These data collectively indicate that ephrinB2 transduces signals inhibiting osteoclast differentiation.

Overexpression of ephrinB2 inhibits osteoclastogenesis

We further examined the role of ephrinB2 in osteoclast differentiation by gain-of-function experiments. Infection of bone marrow cells with a retroviral vector expressing wild-type ephrinB2 suppressed formation of large multinucleated osteoclasts when cocultured with ST2 cells, indicating that overexpressed ephrinB2 transduced inhibitory signals into osteoclast precursors (Figure 3A). To determine whether the negative signal was indeed transduced through the ephrinB2 cytoplasmic domain, we generated ephrinB2 mutants lacking the entire cytoplasmic domain (ΔC) or only the highly conserved C-terminal 33 amino acids (Δ33). In addition, we generated a deletion mutant lacking only the C-terminal YKV (ΔYKV), which interacts with PDZ domains, and a mutant with six tyrosine-to-phenylalanine substitutions in the cytoplasmic domain (Y6F) (Figure 3B). The ΔC and Δ33 constructs were synthesized and properly expressed on the cell surface, based on observations that the extracellular domains of both were recognized by an anti-ephrinB2 antibody (Figure 3C and Figure S3A) and that ΔC and Δ33 overexpression stimulated osteoblast differentiation in vitro (see Figure 5B). As expected, neither ΔC nor Δ33 suppressed formation of

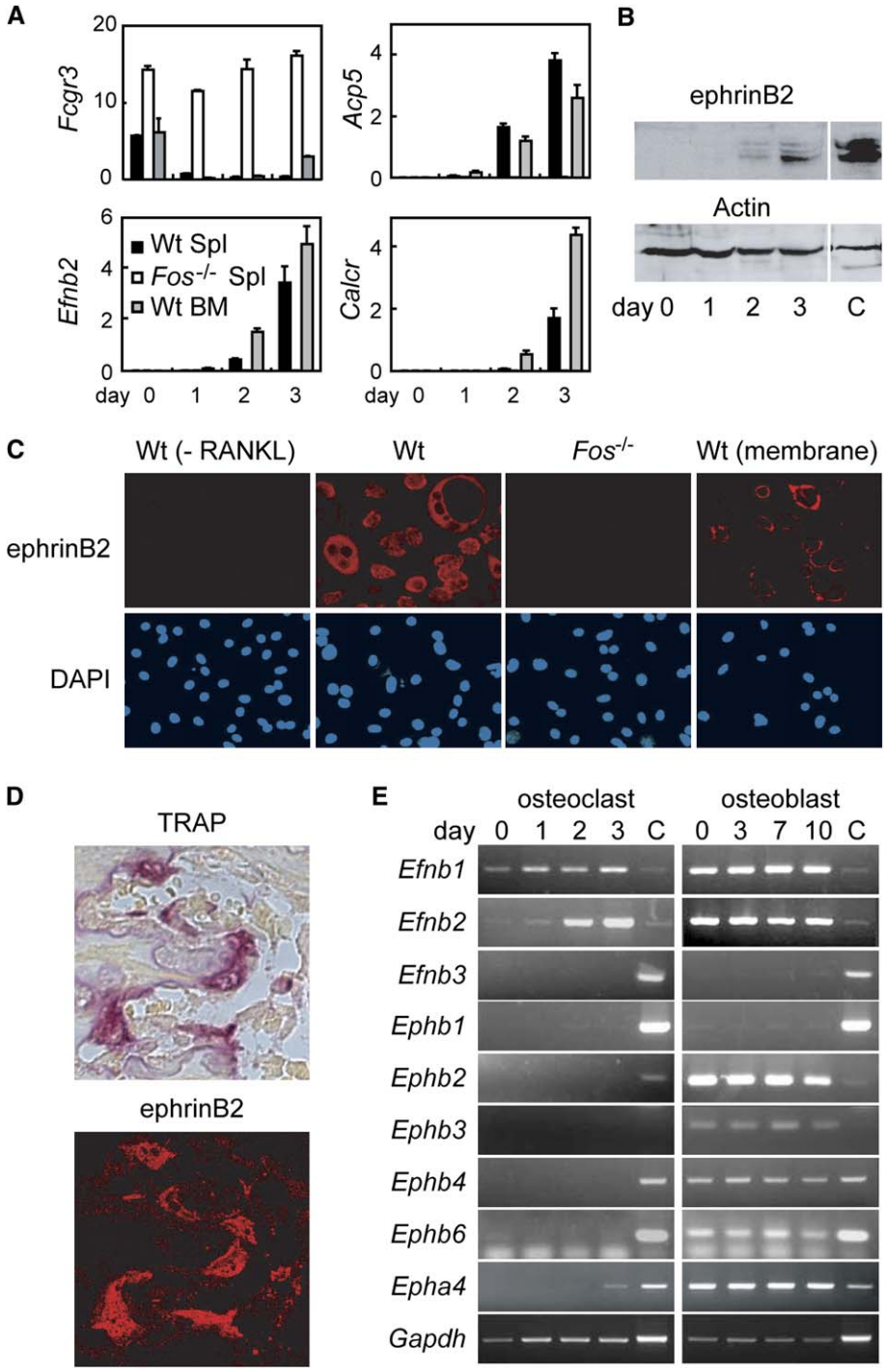

Figure 1. Expression of ephrins and Ephs in osteoclasts and osteoblasts

A) Quantitative RT-PCR analysis of gene expression in wild-type (Wt) and *Fos*$^{-/-}$ osteoclast precursors (MDMs; see Experimental Procedures) in the presence of RANKL. Spl, spleen; BM, bone marrow. Bars represent means ± SEM.

B) Immunoblot analysis of ephrinB2 during osteoclast differentiation of wild-type MDMs. Actin serves as a loading control. C, control expressing exogenous ephrinB2.

C) Immunofluorescence of ephrinB2 in wild-type MDMs treated with RANKL for 3 days. Negative controls are wild-type MDMs in the absence of RANKL, and *Fos*$^{-/-}$ MDMs in the presence of RANKL. "Wt (membrane)" indicates that immunostaining was performed before cell fixation and permeabilization. Nuclei were stained with DAPI (blue) as shown in lower panels.

D) Expression of ephrinB2 in bone. Upper panel, TRAP-activity staining (TRAP). Lower panel, immunofluorescence of ephrinB2 in tibia.

E) RT-PCR analysis of ephrins and Ephs in MDMs and calvarial osteoblasts during differentiation. C, control adult mouse brain.

multinucleated giant cells when infected bone marrow cells were cocultured with ST2 cells, demonstrating that the intracellular domain of ephrinB2 is essential for reverse signaling. Importantly, the ΔYKV but not the Y6F mutant lacked inhibitory activity, strongly suggesting that interaction with PDZ domain proteins, but not tyrosine phosphorylation, mediates the inhibitory signals (Figure 3B). Similar results were obtained in stromal cell-free cultures (data not shown). These data indicate that the cytoplasmic domain of ephrinB2 transduces the inhibitory effect and that the C-terminal YKV is critical for signal transduction.

Loss of reverse signaling enhances osteoclastogenesis

We next examined the role of ephrinB2 during osteoclastogenesis by loss-of-function experiments. First, we knocked down endogenous *Efnb2* transcripts by small interfering RNA (siRNA) using the retroviral vector RVH1 (Barton and Medzhitov, 2002). Retroviral gene transfer and immunoblot analysis confirmed that the knockdown vector efficiently inhibited *Efnb2* expression in M-CSF-dependent bone marrow-derived macrophages treated with RANKL for 3 days (Figure 3D, upper). Green fluorescent protein (GFP)-positive bone marrow cells, which had been

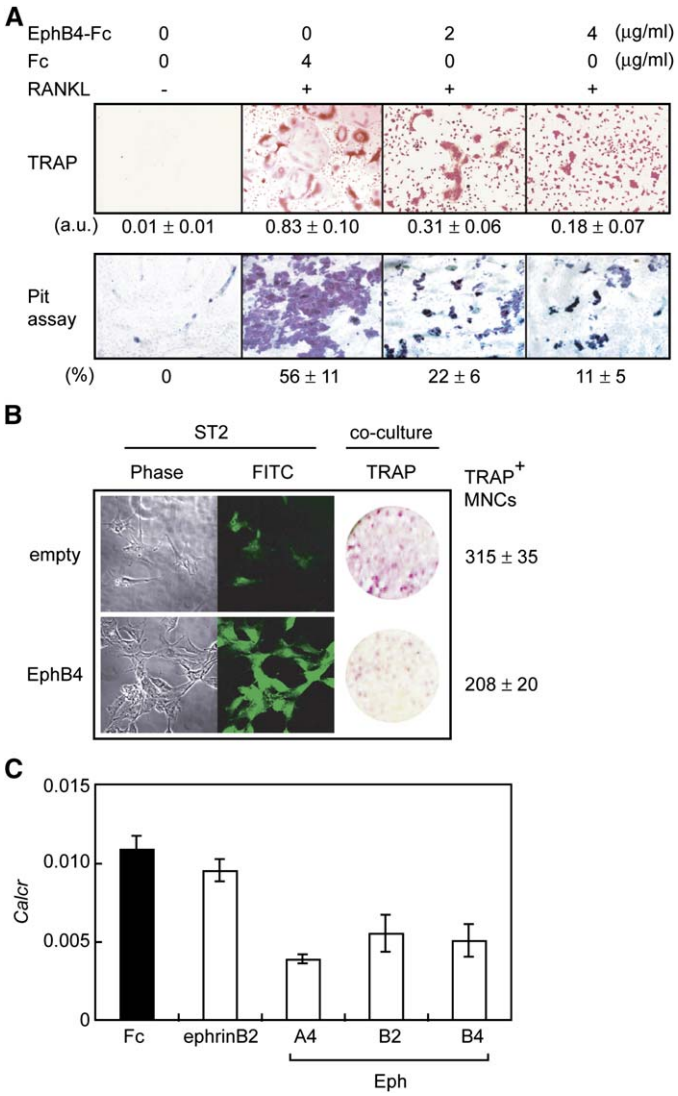

Figure 2. Reverse signaling through ephrinB2 inhibits osteoclast differentiation

A) Treatment of MDMs with clustered EphB4 or control Fc at indicated concentrations in the presence of RANKL (10 ng/ml). Upper panels, TRAP staining after 5 days. Values represent relative TRAP activities in cell lysates. a.u., arbitrary units. Lower panels, resorption pits on bovine bone slices after culturing in the presence of RANKL for 7 days; values represent bone surface resorbed (%).

B) Overexpression of EphB4 in ST2 cells suppresses osteoclast differentiation. Receptor body staining using ephrinB2-Fc, and fluorescein-isothiocyanate (FITC)-conjugated anti-Fc antibody confirmed higher levels of EphB4 expression in transfected ST2 cells (FITC). After coculturing with wild-type bone marrow cells, TRAP-positive multinucleated cells (MNCs) were counted. Values represent means ± SD.

C) Quantitative RT-PCR analysis of *Calcr* expression during RANKL-induced osteoclast differentiation of wild-type MDMs on coverglasses coated with EphA4-Fc, EphB2-Fc, or EphB4-Fc (day 6). Fc and ephrinB2-Fc were included as negative controls. Bars represent means ± SEM.

infected with the siRNA virus, were sorted and cocultured with ST2 cells. After 5 days, ephrinB2 knockdown cultures displayed increased numbers of well-differentiated osteoclasts (Figure 3D, lower). Next, we isolated bone marrow cells from conditional ephrinB2 knockout mice (Gerety and Anderson, 2002) carrying the LysMcre allele (Clausen et al., 1999), which deletes the floxed *Efnb2* loci (*Efnb2*$^{f/f}$) in a myeloid lineage. Deletion of *Efnb2* was confirmed by genomic PCR analysis in M-CSF-dependent bone marrow-derived macrophages (Figure 3E and Figure S3B). Furthermore, *Efnb2* induction was abolished in *Efnb2*$^{f/f}$ cells in the presence of the LysMcre allele (Figure 3F), and these cells showed more efficient osteoclast formation compared to control cells without the deletion (Figure 3G). Therefore, both gain- and loss-of-function experiments demonstrated that ephrinB2 signaling suppresses osteoclast formation in vitro.

To evaluate in vivo effect of *Efnb2* deletion, we also analyzed femurs and tibias of mice lacking ephrinB2 in the macrophage-osteoclast lineage. Although osteoclast number was very slightly increased, bone volume, osteoblast surface (% of bone surface), and the bone mineral density (BMD) of conditional ephrinB2 knockout mice (*Efnb2*$^{f/f}$, Cre^{+}) were comparable to that of controls (*Efnb2*$^{f/f}$, Cre^{-}) (Figures S3C and S3D), suggesting that ephrinB1 or other compensatory factors can maintain bone homeostasis in vivo in the absence of ephrinB2 in the osteoclast lineage.

Reverse signaling inhibits *Fos* and *Nfatc1* expression

We next determined whether inhibitory signaling downstream of ephrinB2 affects expression of two pivotal osteoclastogenic transcription factors, c-Fos and NFATc1. Immunoblot analysis showed that treatment with EphB4 suppressed induction of c-Fos on day 2 and NFATc1 on day 4 (Figure 4A). Levels of *Fos* and *Nfatc1* transcripts, as well as the numbers of TRAP-positive multinucleated cells, were reduced in bone marrow cells in the presence of EphB4 under osteoclastogenic conditions (Figure 4B). Furthermore, expression of *Fcgr3*, which was high in *Fos*$^{-/-}$ osteoclast precursors (Figure 1A), was elevated in the presence of EphB4 (Figure 4B). These data suggest that ephrinB2 signaling inhibits osteoclastogenesis by blocking induction of *Fos* and its transcriptional target *Nfatc1*. To confirm these findings, we retrovirally introduced c-Fos and NFATc1 into bone marrow cells and cultured them with EphB4 in the presence of M-CSF and RANKL. EphB4 suppressed formation of large multinucleated cells from bone marrow cells infected with empty virus. In contrast, bone marrow cells infected with c-Fos virus were insensitive to suppression by EphB4 and formed well-differentiated large osteoclasts (Figure 4C). Infection with NFATc1 virus also conferred resistance to EphB4 treatment (Figure 4D). Therefore, inhibition of *Fos* and *Nfatc1* transcription is one mechanism by which reverse signaling through ephrinB2 suppresses osteoclast differentiation.

Forward signaling enhances osteoblast formation

Apart from the reverse signaling into osteoclasts through ephrinB2, ephrinB2-EphB4 interaction between osteoclasts and osteoblasts must simultaneously transmit signals in the opposite direction, namely, as forward signaling through EphB4 into osteoblasts. The addition of clustered ephrinB2 to osteoblastogenic cultures significantly stimulated differentiation of calvarial osteoblasts, as judged from alkaline phosphatase (ALP) staining, and clustered soluble EphB4 neutralized this stimulatory effect (Figure 5A). Overexpression of ephrinB2 in osteoblasts by retroviral gene transfer also stimulated osteoblast differentiation (Figure 5B). This stimulatory effect was independent of the ephrinB2 cytoplasmic domain, given that wild-type, ΔC, and Δ33 mutants all enhanced ALP staining (Figure 5B), and supports the idea that it is the ephrinB2 extracellular domain that stimulates Eph receptors. Quantitative RT-PCR analysis showed that when stimulated with clustered ephrinB2, expression of

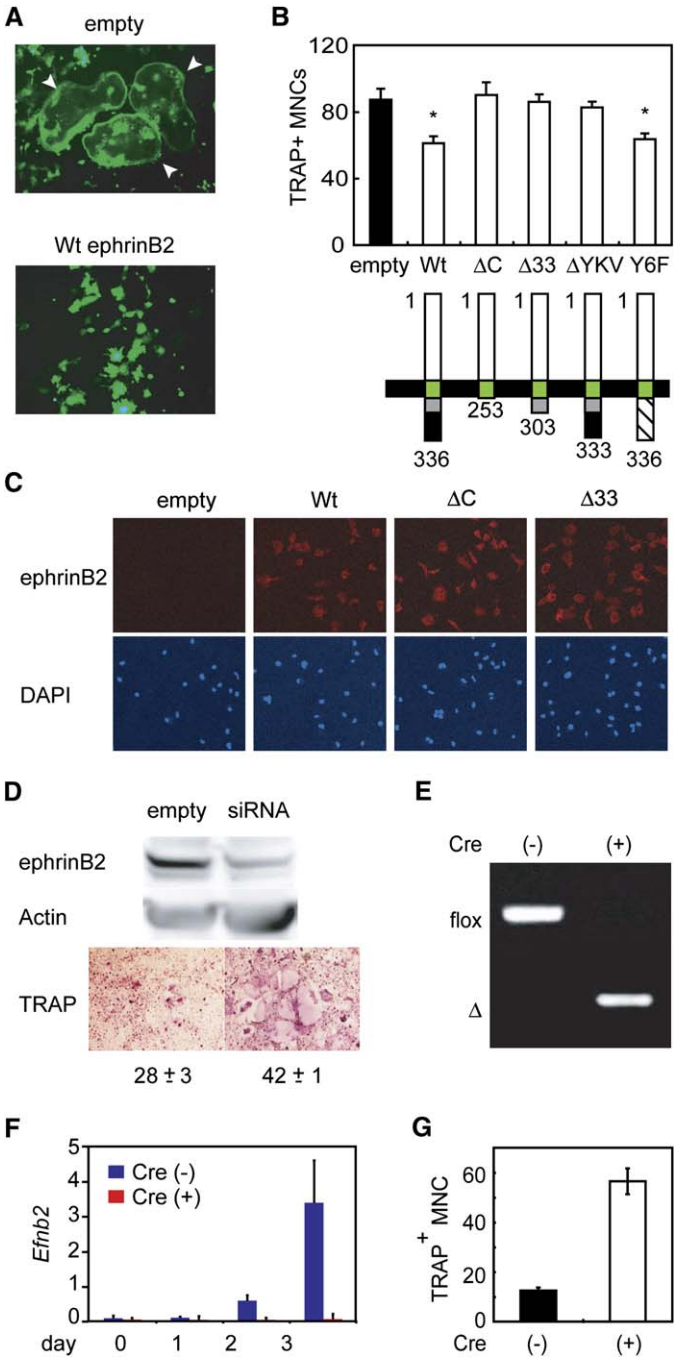

Figure 3. Gain- and loss-of-function of ephrinB2 in osteoclasts

A) MDMs were infected with the expression viruses pMX-IRES-GFP (empty) or pMX-ephrinB2-IRES-GFP (Wt ephrinB2) and cocultured with ST2 cells for 6 days. Arrowheads, GFP-positive multinucleated cells (MNC).

B) Upper, number of large (>65 μm), TRAP-positive MNCs (means ± SEM) determined after overexpression of Wt ephrinB2 and mutants. Lower, schematic representation of Wt and mutant constructs.

C) Upper panels, immunofluorescence of extracellular domains of retrovirally expressed ephrinB2 mutants (ΔC and Δ33) in MDMs. Immunostaining was performed before cell fixation and permeabilization. Lower panels, DAPI staining of the same culture. Experiment was performed as in Figure 1C.

D) Knockdown of ephrinB2. Upper, immunoblot analysis of ephrinB2 after retroviral gene-transfer of RVH1-GFP (empty) and RVH1-siRNA-GFP (siRNA) vectors into wild-type MDMs, followed by RANKL treatment for 3 days. Lower, TRAP staining of cocultures containing sorted GFP-positive MDMs infected with empty or siRNA viruses (TRAP). Numbers represent TRAP-positive giant MNCs in triplicate 24-well samples (means ± SEM).

E) Genomic PCR analysis of *Efnb2* deletion in MDMs isolated from *Efnb2*$^{f/f}$ mice without (−) or with (+) the LysMCre allele. The 636 bp (flox) and 309 bp (Δ) bands represent floxed and deleted *Efnb2* loci, respectively.

F) Quantitative RT-PCR analysis of *Efnb2* during osteoclast differentiation of MDMs described in (**E**). Bars represent means ± SD.

G) Number of TRAP-positive MNCs (means ± SEM) in 5 day cocultures containing MDMs described in (**E**) and ST2 cells.

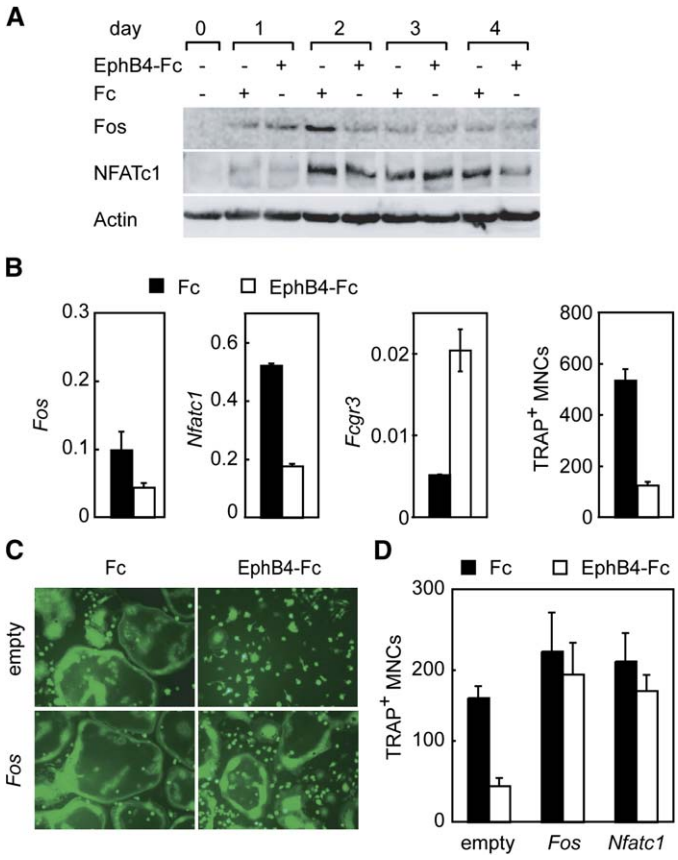

Figure 4. Reverse signaling inhibits expression of c-Fos and NFATc1

A) Immunoblot analysis of c-Fos and NFATc1 during osteoclast formation in the presence of clustered Fc or EphB4-Fc (2 μg/ml).

B) Quantitative RT-PCR analysis of the expression of *Fos* (day 2), *Nfatc1* (day 4), and *Fcgr3* (day 4), and number of TRAP-positive MNCs (day 4) in the presence of clustered Fc or EphB4-Fc in stromal cell-free cultures. Bars represent means ± SD.

C) EphB4 treatment of MDMs overexpressing c-Fos. MDMs were infected with pMX-IRES-GFP (empty) or pMX-Fos-IRES-GFP (Fos) and cultured without or with EphB4-Fc (2 μg/ml).

D) Number of TRAP-positive MNCs in 4 day osteoclastogenic cultures in the presence of Fc or EphB4-Fc. MDMs were infected with pMX-IRES-GFP (empty), pMX-Fos-IRES-GFP (Fos), or pMSCV-NFATc1-IRES-GFP (NFATc1) prior to osteoclastogenesis. Bars represent means ± SD.

osteoblast differentiation markers, such as *Alp*, *Col1* (*Col1a1*, collagen Iα), and *Og2* (osteocalcin), was increased (Figure 5C). Consistently, mRNAs encoding transcription factors critical for osteoblast differentiation, such as *Dlx5* (distal-less homeobox 5), *Osx* (osterix, also known as *Sp7*) (Nakashima et al., 2002), and *Runx2* (runt-related transcription factor 2, also known as Cbfa1) (Ducy et al., 1997; Komori et al., 1997), were significantly induced by ephrinB2 (Figure 5C). We knocked down *Ephb4* expression by introducing siRNA vectors into calvarial osteoblasts

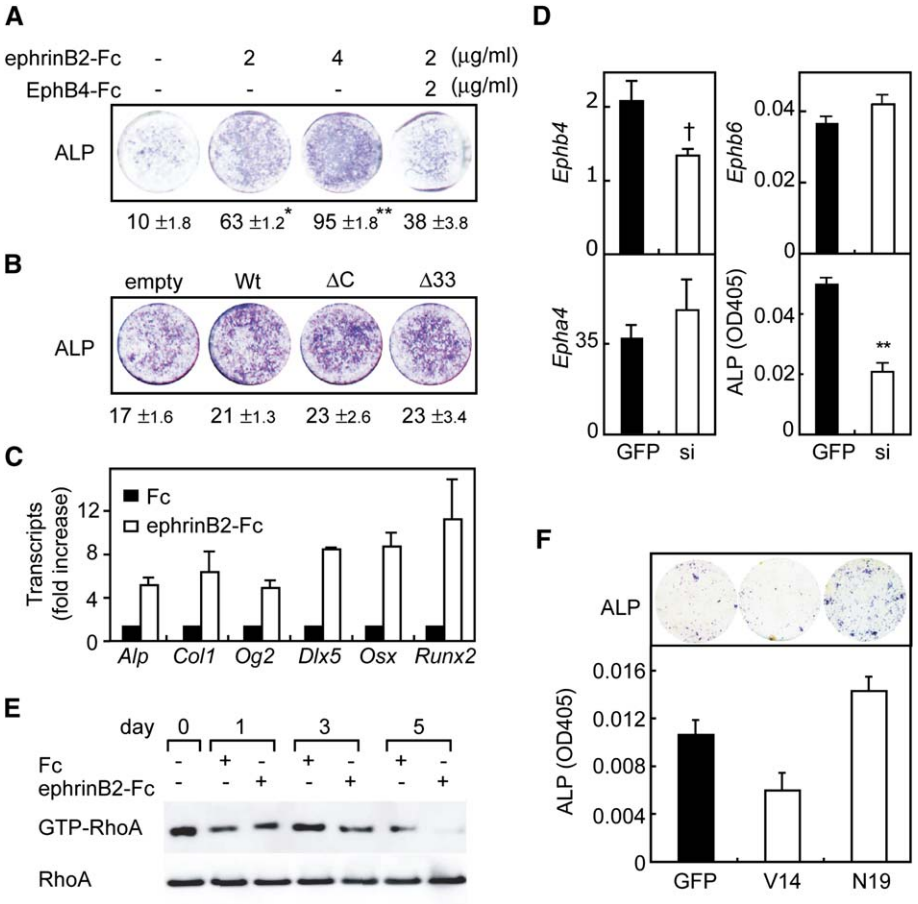

Figure 5. Forward signaling through EphB4 enhances osteoblast differentiation

A) ALP staining of osteoblasts in osteoblastogenic cultures containing indicated concentrations of clustered ephrinB2 and EphB4 for 6 days. Two independent preparations of osteoblasts showed similar results. Staining intensity was quantified with Image J. *p < 0.05, **p < 0.01, versus no treatment. Bars represent means ± SEM.

B) ALP staining of osteoblasts 6 days after infection with wild-type (Wt) and mutant ephrinB2 viruses (ΔC and Δ33). Bars represent means ± SEM.

C) Quantitative RT-PCR analysis of osteoblasts cultured under osteoblastogenic conditions in the presence of ephrinB2-Fc. RNAs were prepared on day 6 (for *Alp*, *Dlx5*, *Osx*, and *Runx2*) and on day 9 (for *Col1* and *Og2*). Bars represent means ± SD.

D) EphB4 knockdown experiment. Quantitative RT-PCR analysis of *Ephb4* in osteoblasts differentiated in the presence of ephrinB2 for 9 days after infecting with siRNA virus (si) or a GFP virus. *Ephb6* and *Epha4* were evaluated to examine the specificity of *Ephb4* siRNA. ALP activity in lysates was also quantified. †p = 0.063, **p < 0.01 versus GFP virus. Bars represent means ± SEM.

E) Immunoblot analysis of RhoA activity in osteoblasts stimulated with Fc or ephrinB2-Fc for the indicated days.

F) Effect of RhoA activity on osteoblast differentiation. V14, constitutively active RhoA; N19, dominant-negative RhoA. Upper, ALP staining (day 6) of calvarial osteoblasts. Lower, ALP activity in lysates. Bars represent means ± SEM.

and differentiated them into mature osteoblasts in the presence of ephrinB2. The siRNA vector reduced *Ephb4* transcripts and lowered ALP activity, whereas irrelevant *Epha4* and *Ephb6* transcripts were not affected, indicating that signaling from EphB4 specifically stimulates osteoblast differentiation (Figure 5D).

We examined potential downstream effectors of forward signaling in osteoblasts stimulated with ephrinB2. During in vitro differentiation of osteoblasts, phosphorylation of ERK1/2 was enhanced (Figure S4), which may lead to stimulation of osteoblast differentiation. We also analyzed the active guanosine triphosphate (GTP) bound form of the small GTPase RhoA (Etienne-Manneville and Hall, 2002) since inhibition of Rho-Rho kinase signaling stimulates differentiation of mouse calvarial osteoblasts (Harmey et al., 2004). GTP-RhoA was reduced by ephrinB2 treatment (Figure 5E). To ask whether RhoA activity negatively regulates osteoblast differentiation, we introduced by retroviral gene transfer a constitutively active (V14) or a dominant-negative (N19) form of RhoA (Gebbink et al., 1997) into osteoblasts in culture. After 6 days, RhoA (V14) suppressed ALP activity and RhoA (N19) enhanced it (Figure 5F), indicating that RhoA inactivation is a mechanism by which forward signaling through EphB4 enhances osteoblast formation.

Enhanced bone formation in EphB4 transgenic mice

To examine the effects of forward signaling through EphB4 on bone homeostasis in vivo, we generated EphB4 transgenic mice, in which EphB4 is expressed in osteoblasts under the control of the mouse *Col1* promoter (Liu et al., 2001). Overexpression of EphB4 in transgenic osteoblasts was confirmed by immunohistochemical staining of sections of femur (Figure 6A) and tibia (Figure 6B). To compare expression levels of *Ephb4* between wild-type and EphB4 transgenic mice, we performed quantitative RT-PCR using RNA prepared from calvaria, femur, and tibia. On average, EphB4 transgenic mice expressed 6.7-fold higher levels of *Ephb4* transcripts in calvaria and 4.8-fold higher in the long bones (Figure 6C). We next compared *Ephb4* transcripts using cultured calvarial osteoblasts and bone marrow-derived osteoclasts. EphB4 transgenic osteoblasts expressed a 5.2-fold higher level of *Ephb4* than wild-type controls, whereas osteoclasts did not express detectable *Ephb4* from the transgene (Figure 6D). These calvarial osteoblasts isolated from EphB4 transgenic mice differentiated more efficiently than those from wild-type controls, as judged from both ALP and Alizarin Red staining (Figure 6E).

Radiographs and microcomputed tomography (μCT) revealed that EphB4 transgenic mice exhibited increased bone mass by 10 weeks of age (Figure 7A). Dual energy X-ray absorptiometry (DEXA) showed that the BMD of femurs from transgenic mice was consistently greater than that of wild-type controls (Figure 7B). Quantitative bone histomorphometry further showed that bone volume, osteoid thickness, mineralizing surface, and bone formation rate were significantly increased in transgenic mice versus wild-type controls (Figure 7C). Serum levels of osteocalcin, a marker of bone formation, were also slightly elevated in EphB4 transgenic mice (Figure 7D). Strikingly, osteoclast number, osteoclast surface, and eroded surface were

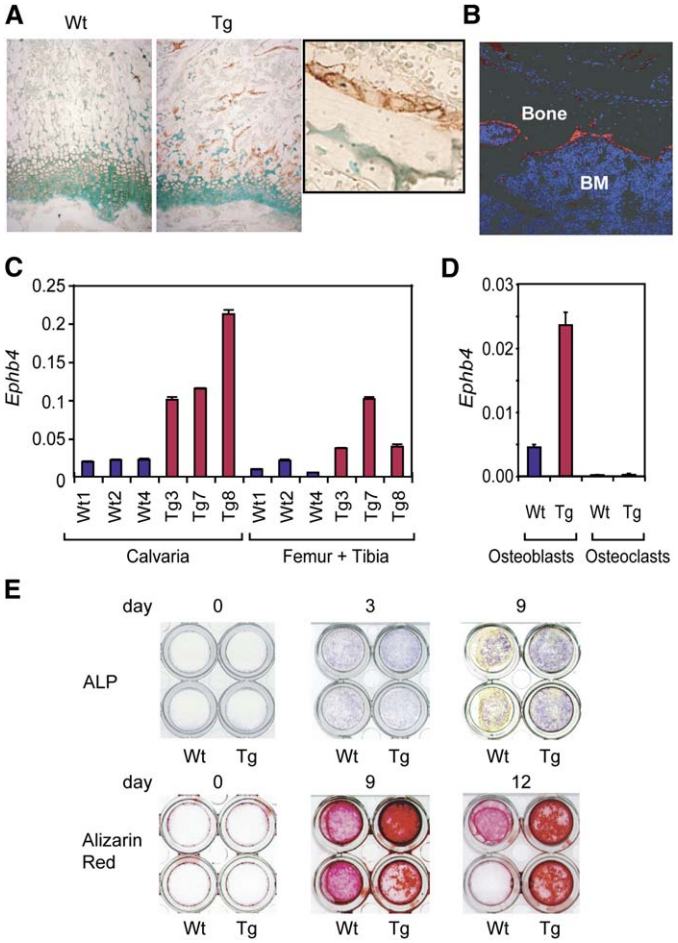

Figure 6. Expression of EphB4 in transgenic mice and in vitro osteoblast differentiation

A) Immunohistochemical staining of EphB4 (red) in distal femurs from 8-week-old, wild-type (Wt) and transgenic (Tg) mice. Counterstaining, methyl-green. Orientation is as in Figure 7A.

B) Immunofluorescence detection of EphB4 (red) in tibia from 8-week-old transgenic mice. Counterstaining, DAPI (blue). BM, bone marrow.

C) Quantitative RT-PCR analysis of *Ephb4* expression. Total RNA was isolated directly from calvaria and femur + tibia. *Ephb4* transcripts in individual Wt and EphB4 Tg mice (n = 3 for each genotype) were separately measured. Bars represent means ± SEM.

D) Quantitative RT-PCR analysis using calvarial osteoblasts and bone marrow-derived osteoclasts prepared from Wt and EphB4 Tg mice. Bars represent means ± SEM.

E) In vitro osteoblastogenesis of EphB4-expressing osteoblasts. Duplicate cultures were terminated on the days indicated and stained for ALP activity or with Alizarin red.

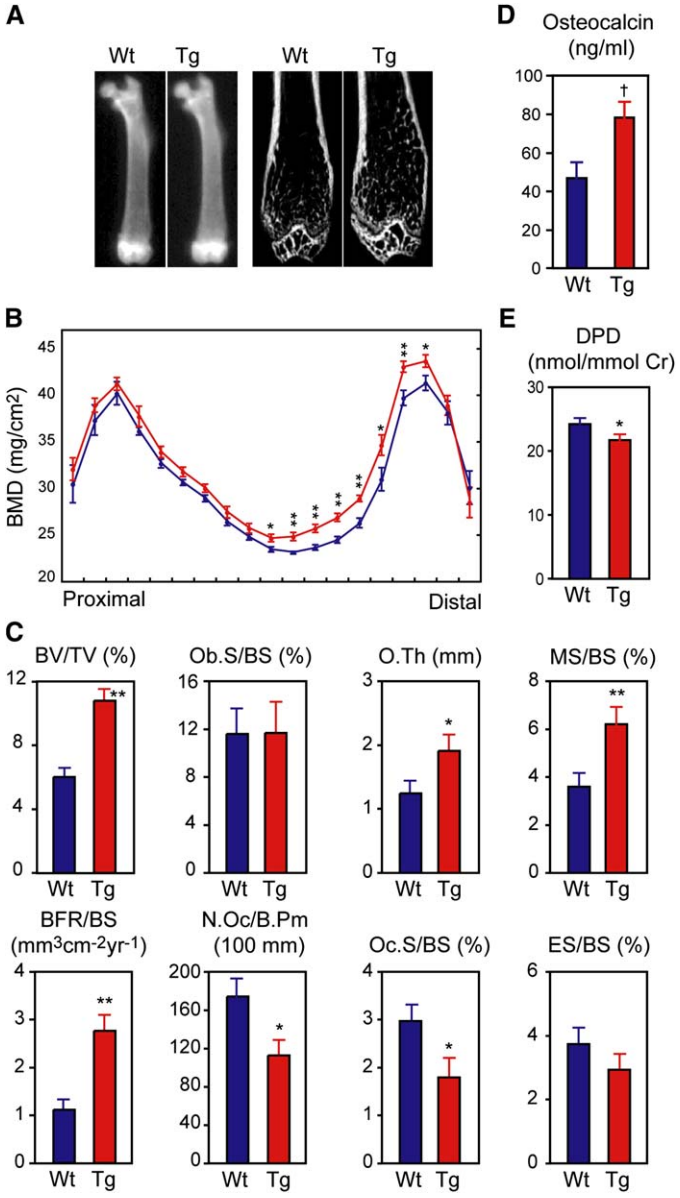

Figure 7. EphB4 transgenic mice show increased bone mass

A) Radiographic analysis (left panels, radiograph; right panels, μCT) of femurs from 10-week-old mice.

B) Quantification of BMD of femurs isolated from 10-week-old female mice by DEXA (Wt n = 6, Tg n = 10, data shown as means ± SEM, *p < 0.05, **p < 0.01).

C) Histomorphometrical analysis of tibia from 10-week-old mice (each group n = 8, data shown as means ± SEM, *p < 0.05, **p < 0.01). BV/TV, bone volume per tissue volume; Ob.S/BS, osteoblast surface per bone surface; O.Th, osteoid thickness; MS/BS, mineralizing surface per bone surface; BFR/BS, bone formation rate per bone surface; N.Oc/B.Pm, osteoclast number per bone perimeter; Oc.S/BS, osteoclast surface per bone surface; ES/BS, eroded surface per bone surface.

D) Serum osteocalcin levels (†p < 0.07) in Wt and Tg mice. Bars represent means ± SEM.

E) Urinary deoxypyridinoline (DPD) measurement in Wt and Tg mice. (Wt n = 22, Tg n = 16, *p < 0.05). Bars represent means ± SEM.

significantly reduced in EphB4 transgenic mice compared to wild-type controls, indicating that osteoclast function was inhibited in these mice (Figure 7C). Consistently, EphB4 transgenic mice showed a decrease in urinary deoxypyridinoline (DPD) crosslinks, a marker for osteoclastic bone resorption, indicating that osteoclast function was suppressed (Figure 7E). Such reduced osteoclastic activity is not due to reduction in RANKL or M-CSF or to an increase in OPG since there was no significant difference in *Rankl*, *Csf1*, and *Opg* mRNA levels in bone or RANKL and OPG levels in serum between wild-type and EphB4 transgenic mice (data not shown). Since EphB4 binds only to ephrinB2 (Gale and Yancopoulos, 1999; Myshkin and Wang, 2003), we conclude that the results of the bone histomorphometric analysis are a consequence of direct interaction between EphB4 and ephrinB2. Collectively, elevated levels of EphB4 in osteoblasts not only enhance bone formation but also inhibit bone resorption in vivo.

Discussion

The interaction between ephrins and Ephs has been extensively investigated in neural development, angiogenesis, skeletal patterning, and other contexts (Compagni et al., 2003; Davy et al., 2004; Himanen and Nikolov, 2003; Kullander and Klein, 2002; Murai and Pasquale, 2003; Palmer and Klein, 2003). However, roles for ephrin-Eph bidirectional signaling in bone remodeling have not been demonstrated. In this study, we show that ephrinB2 and EphB4 regulate differentiation of osteoclasts and osteoblasts, suppressing bone resorption and enhancing bone formation. Our results indicate that ephrinB2 expression is dependent on a RANKL-induced c-Fos-NFATc1 transcriptional cascade during osteoclast differentiation. On the other hand, EphB4 expression is constitutive and the forward signaling through EphB4 induces osteogenic regulatory factors, such as *Dlx5*, *Osx*, and *Runx2*, in calvarial osteoblasts, suggesting that EphB4 is at the top of the regulatory cascade during osteoblast differentiation.

We observed that reverse signaling through ephrinB2 into hematopoietic precursors suppresses osteoclast differentiation. Although ephrin-Eph signaling frequently decreases cell adhesion in various cell types, we did not observe decreased adhesion (increased detachment) of osteoclast precursors stimulated with EphB4 (data not shown). Therefore, the observed inhibitory effects of ephrinB2 are not due to a loss of osteoclast precursors from the culture. How then does ephrinB2 reverse signaling suppress osteoclast differentiation? Our data indicate that such suppression requires the ephrinB2 C-terminal YKV motif, suggesting the involvement of as yet unidentified PDZ domain proteins in mediating the signal. Although how signals downstream of M-CSF or RANKL are abrogated in these cells remains unknown, transcription of *Fos* and its target *Nfatc1* is inhibited by the ephrinB2 reverse signaling, and overexpression of c-Fos or NFATc1 relieves the inhibitory effect. Therefore, the osteoclastogenic c-Fos-NFATc1 cascade is controlled by a negative feedback loop through ephrinB2.

Bidirectional ephrin-Eph signaling links the negative feedback loop in osteoclast differentiation to positive regulation of osteoblast differentiation, thereby maintaining bone homeostasis. By overexpressing EphB4, we showed that forward signaling through EphB4 enhances osteoblast differentiation both in cultured cells and in mice. Consistently, knockdown of EphB4 signaling by siRNA resulted in reduced osteoblast differentiation. EphB receptors are known to interact with various signaling pathways (Pasquale, 2005), including those requiring the activity of Src, PI3K-Akt (Steinle et al., 2002), and the Ras/Rho families of small molecular weight GTPases (Noren and Pasquale, 2004). We showed that EphB4 signaling activated ERK1/2 pathways, which may explain enhanced osteoblast differentiation (Jaiswal et al., 2000; Wang et al., 2002; Xiao et al., 2000). We also observed that EphB4 signaling attenuates RhoA activity. Although this is in agreement with the notion that higher RhoA activity inhibits osteoblast differentiation (Harmey et al., 2004), McBeath et al. (2004) using human mesenchymal stem cells suggest that active RhoA enhances osteoblast differentiation. In mouse primary calvarial osteoblasts, a constitutively active form of RhoA inhibited and a dominant-negative form of RhoA stimulated osteoblast differentiation, supporting the notion that EphB4-forward signaling enhances osteoblast differentiation by lowering RhoA activity. Whether and how EphB4-forward signaling critically affects ERKs, RhoA, or other heterologous signaling pathways should be determined by future pharmacological or genetic studies.

Transgenic mice overexpressing EphB4 showed increased femoral bone density. Although the bone formation rate was elevated in transgenic mice, the osteoblast surface was not significantly increased in these mice, suggesting that osteoblast function may be enhanced in transgenic mice. On the other hand, EphB4 transgenic mice showed a reduction in osteoclast number and osteoclast surface, suggesting that reverse signaling through ephrinB2 into osteoclasts was increased by forced expression of EphB4 in vivo. Furthermore, the decrease in urinary DPD crosslinks provides additional support for the idea that reverse signaling into osteoclasts through ephrinB2 is enhanced in EphB4 transgenic mice. Since a reduced number of osteoclasts should lead to overall reduction in forward signaling in osteoblasts, the net result of EphB4 overexpression on bone metabolism in vivo would be complex compared to EphB4 overexpression in cultured osteoblasts stimulated with soluble ephrinB2.

Why do conditional knockout mice lacking ephrinB2 in the myeloid lineage not exhibit a strong bone phenotype? The nature of reverse signaling of ephrinB1 and ephrinB2 is likely to be similar because the amino acid sequence of their intracellular domains is highly conserved. This implies that upon Eph binding, ephrinB1, which is also expressed in differentiating osteoclasts, signals in a manner similar ephrinB2. Since EphB4 does not interact with ephrinB1, other Eph receptors such as EphB2 or EphB3, which are also expressed in osteoblasts, may interact with ephrinB1. Eph receptors other than EphB4 likely compensate for forward signaling mediated by EphB4 in the absence of ephrinB2.

In contrast to what we show in this study, the word ''coupling'' traditionally refers to the positive correlation between systemic bone resorption and bone formation (Harris and Heaney, 1969). Our finding is consistent with such ''coupling'' when each bone remodeling cycle is considered at a microscopic level. To achieve coupling, termination of osteoclastic bone resorption has to be followed by osteoblastic bone formation, which refills resorption lacunae with new bone (Hattner et al., 1965; Parfitt, 1994). We suggest that a bidirectional interaction between ephrinB ligands expressed on osteoclasts and Eph receptors on osteoblasts can dynamically enhance the transition from resorption to a reversal phase occurring at each resorption cycle (Parfitt, 1994), when osteoclast activity is attenuated and osteoblasts initiate bone formation at resorption lacunae. Then, an osteoclast-free area might be maintained by ephrinB reverse signaling to osteoclast precursors. Furthermore, continuous bone formation by osteoblasts over the several months required to refill resorption lacunae might be self-maintained by ephrin-Eph interactions on osteoblasts. This study establishes the concept that ephrin-Eph signaling contributes to bone homeostasis.

Experimental procedures

Mice

Mouse *Ephb4* cDNA was subcloned into the NotI site of modified pNASSβ, which contains the 2.3 kb osteoblast-specific promoter region for the mouse pro-α1 (I) collagen gene (Liu et al., 2001). The NarI-SalI fragment containing the 2.3 kb pro-α1 (I) promoter-*Ephb4* coding region-poly (A) signal was isolated and microinjected into pronuclei of fertilized eggs from B6C3F1 (C57BL/6 × C3H/He) females. $Fos^{-/-}$ mice were produced by mating $Fos^{+/-}$ mice on a 129 × C57BL/6 mixed background (Wang et al., 1992).

To specifically delete ephrinB2 in myeloid cells, conditional ephrinB2 knockout mice (Gerety and Anderson, 2002) and LysMcre mice (Clausen et al., 1999) were crossed. All animals were treated in accordance with the guidelines of Keio University for animal and recombinant DNA experiments.

Bone phenotype analysis

Bone mineral density was measured with DEXA (DCS-600R, Aloka) and quantitative computed tomography (LaTheta, Aloka). Bone histomorphometry and urinary DPD measurement were performed as described (Nishiwaki et al., 2006). Osteocalcin was quantified with an ELISA kit (Biomedical Technologies). Bone tissues and cultured cells were immunostained using polyclonal anti-EphB4 goat (R&D), polyclonal anti-ephrinB2 goat (R&D), and Alexa647-conjugated anti-goat chicken (Invitrogen) antibodies. Fluorescent images were acquired using a Fluoview1000 (Olympus) confocal microscope.

Bone resorption assay

Bone slices were prepared from diaphysis of bovine long bones cut out with a band saw. The diaphysis tube was cut longitudinally into pieces, and bone marrow and soft tissue were removed under running water. Blocks of cortical bone were immersed in xylene for 30 min, transferred to alcohol for 30 min, dried overnight in oven at 45°C, and sliced with a diamond saw (Isomet, Buehler). Slices were washed three times in water, sonicated for 10 min, washed three times in water, immersed in acetone for 10 min, washed in alcohol twice, drained, and dried in air. The bone slices were placed in the bottom of wells and cells were cultured on top of bone slices. Cells on bone slices were removed in 10% sodium hypochlorite. Air dried bone slices were stained with hematoxylin. The entire surface of each bone slice was examined and the total area resorbed per bone slice was quantified blind using ImageJ (National Institutes of Health).

Plasmid constructions

ΔC (deletion of entire cytoplasmic domain), Δ33 (deletion of the last C-terminal 33 amino acids), and ΔYKV were generated by PCR-mediated mutagenesis based on mouse *Efnb2* cDNA and cloned into pMX-IRES-GFP and pcDNA3 (Invitrogen). Y6F (in which all six tyrosines in the cytoplasmic domain were substituted with phenylalanines) was generated using a QuickChange site-directed mutagenesis kit (Stratagene). Expression of mutants was confirmed in COS7 cells by transient transfection and immunoblotting. *Ephb4* cDNA was cloned between the BamHI and XhoI sites of pCMV-Tag4A (Stratagene). Constitutively active RhoA (V14) and dominant-negative RhoA (N19) cDNAs (Gebbink et al., 1997) were cloned into the EcoRI and NotI sites of pMX-IRES-GFP. Inserts were verified by DNA sequencing. Retroviral *Efnb2* siRNA vectors were constructed in RVH1 (Barton and Medzhitov, 2002). The CD4 cDNA of RVH1 was replaced by GFP to generate RVH1-GFP.

Efnb2 siRNA sequences were:

5′-GATCCCCGAATTCAGCCCTAACCTCTTTCAAGAGAAGAGGTTAGGGCTGAATTCTTTTTGGAAC-3′ and 5′-TCGAGTTCCAAAAAGAATTCAGCCCTAACCTCTTCTCTTGAAAGAGGTTAGGGCTGAATTCGGG-3′.

Ephb4 siRNA 1 sequences were:

5′-GATCCCCTGAGGTTGCTGCTTTGAATTTCAAGAGAATTCAAAGCAGCAACCTCATTTTTGGAAC-3′ and 5′-TCGAGTTCCAAAAATGAGGTTGCTGCTTTGAATTCTCTTGAAATTCAAAGCAGCAACCTCAGGG-3′.

Ephb4 siRNA 2 sequences were:

5′-GATCCCCAGTGTTCGTTTCCTGAAGATTCAAGAGATCTTCAGGAAACGAACACTTTTTTGGAAC-3′ and 5′-TCGAGTTCCAAAAAAGTGTTCGTTTCCTGAAGATCTCTTGAATCTTCAGGAAACGAACACTGGG-3′.

Cell culture

For stromal cell-free osteoclast formation, MDMs (Ray et al., 2006) were used as osteoclast precursors. Briefly, total bone marrow cells were flushed out from wild-type femurs or tibias and were cultured overnight in tissue culture dishes in α-minimal essential medium (α-MEM) containing 10% FCS. Nonadherent bone marrow cells were plated at a density of 1×10^5 per 24-well plate or 5×10^4 cells per 48-well plate in α-MEM containing 10 ng/ml of M-CSF (R&D). Three days later, cultures were washed once with phosphate-buffered saline and adherent cells were used as MDMs. *Fos*$^{-/-}$ MDMs were prepared from splenocytes. With or without retroviral infection, MDMs were induced to differentiate into osteoclasts in the presence of 10 ng/ml each of M-CSF and RANKL (R&D) for 3 days. Adherent cells were fixed with 4% paraformaldehyde, treated with ethanol-acetone (50:50), and stained for TRAP activity using a kit (Sigma). TRAP activity in cell lysates was quantified by measuring absorbance at 405 nm using a kit (Sigma). For cocultures, bone marrow cells (nonadherent cells obtained after culturing total bone marrow cells for 18 hr) were seeded at a density of 5×10^5 cells per 48-well plate containing 5×10^4 ST2 cells in 0.35 ml α-MEM supplemented with 10% FCS, 10^{-8} M 1, 25-dihydroxyvitamin D_3, and 10^{-7} M dexamethasone. The medium was changed every 2 days. Mouse primary calvarial osteoblasts were prepared, differentiated, and stained as described (Nishiwaki et al., 2006). Images of wells stained for ALP activity were processed using ImageJ. To establish EphB4-overexpressing stromal cells, ST2 cells (2×10^5) were lipofected with 4 μg of pCMV-EphB4-Tag4A using FuGENE 6 (Roche). Cells were selected in medium containing 500 μg/ml of geneticin (G418). Receptor body staining for EphB4 was as described (Füller et al., 2003). Twelve EphB4 expression clones were obtained and tested for osteoclastogenesis in the coculture system. To stimulate forward or reverse signaling, ephrinB2-Fc, EphA4-Fc, EphB2-Fc, EphB4-Fc, or Fc fragments (R&D) were either clustered with anti-Fc antibody or coated on poly-L-lysine coverglasses at 2 μg/ml unless otherwise indicated.

Retroviral gene transduction

Retroviruses were produced as described (Nishiwaki et al., 2006). Recombinant retrovirus was used to infect primary bone marrow cells or calvarial osteoblasts in the presence of 8 μg/ml polybrene (Sigma).

RT-PCR and quantitative PCR analysis

Total RNA was isolated using Isogen reagent (Nippon Gene) and cDNAs were synthesized using the SuperScript First-Strand Synthesis System for an RT-PCR kit (Invitrogen). RT-PCR primers for *Acp5* and *Calcr* are as described (Matsuo et al., 2004) and others are listed in Table S1. TaqMan RT-PCR primers for *Efnb2, Ephb4, Ephb6, Epha4, Fcgr3, Fos, Gapdh*, and *Nfatc1* were purchased from Applied Biosystems. Values were normalized to *Gapdh*.

Immunoblot analysis

Proteins prepared from osteoclastic or osteoblastic cultures were separated on 4%–12% SDS-polyacrylamide gels (Novex) and transferred onto Hybond nitrocellulose membranes (Amersham). The following primary antibodies were used: polyclonal anti-c-Fos rabbit antibody (Ab-1, Oncogene), a monoclonal anti-NFATc1 mouse antibody (7A6, Santa Cruz), and polyclonal anti-ERK1/2 rabbit and polyclonal anti-ephrinB2 goat antibodies (R&D). Where indicated, blots were stripped and reprobed with a polyclonal anti-actin goat antibody (Santa Cruz) to monitor protein loading. RhoA activity was analyzed by an affinity precipitation assay using a GST-tagged fusion protein of the mouse Rhotekin Rho binding domain (Upstate). GTP-RhoA and total RhoA were detected using a monoclonal anti-RhoA mouse antibody (26C4, Santa Cruz).

Supplemental data

Supplemental data include four figures and one table and can be found with this article online at http://www.cellmetabolism.org/cgi/content/full/4/2/111/DC1/.

Acknowledgments

We thank R. Medzhitov for siRNA vectors, D. Anderson for conditional ephrinB2 knockout mice, I. Förster for LysMcre mice, N. Clipstone for NFATc1 retroviral vectors, H. van Dam for RhoA mutants, H. Murayama, M. Tsuri-Jinno, H. Suzuki, K. Maruyama, and E. Kobayashi for technical assistance, the Central Research Laboratory at Keio University for cell sorting, Y. Toyama for encouragement, and N. Ray, H. Takayanagi, S. Koyasu, L. Bakiri, D. Galson, E.F. Wagner, L. DiMascio, and E. Lamar for critical reading of the manuscript. This work was supported by a Grant-in-Aid for Scientific Research B (17390420) and by Keio Gijuku Academic Development Funds.

Received: December 29, 2005
Revised: April 5, 2006
Accepted: May 12, 2006
Published: August 8, 2006

References

Adams, R.H., Wilkinson, G.A., Weiss, C., Diella, F., Gale, N.W., Deutsch, U., Risau, W., and Klein, R. (1999). Roles of ephrinB ligands and EphB receptors in cardiovascular development: demarcation of arterial/venous domains, vascular morphogenesis, and sprouting angiogenesis. Genes Dev. *13*, 295–306.

Asagiri, M., Sato, K., Usami, T., Ochi, S., Nishina, H., Yoshida, H., Morita, I., Wagner, E.F., Mak, T.W., Serfling, E., and Takayanagi, H. (2005). Autoamplification of NFATc1 expression determines its essential role in bone homeostasis. J. Exp. Med. *202*, 1261–1269.

Barton, G.M., and Medzhitov, R. (2002). Retroviral delivery of small interfering RNA into primary cells. Proc. Natl. Acad. Sci. USA *99*, 14943–14945.

Batlle, E., Henderson, J.T., Beghtel, H., van den Born, M.M., Sancho, E., Huls, G., Meeldijk, J., Robertson, J., van de Wetering, M., Pawson, T., and Clevers, H. (2002). β-catenin and TCF mediate cell positioning in the intestinal epithelium by controlling the expression of EphB/ephrinB. Cell *111*, 251–263.

Clausen, B.E., Burkhardt, C., Reith, W., Renkawitz, R., and Förster, I. (1999). Conditional gene targeting in macrophages and granulocytes using LysMcre mice. Transgenic Res. *8*, 265–277.

Compagni, A., Logan, M., Klein, R., and Adams, R.H. (2003). Control of skeletal patterning by ephrinB1-EphB interactions. Dev. Cell *5*, 217–230.

Cowan, C.A., Yokoyama, N., Saxena, A., Chumley, M.J., Silvany, R.E., Baker, L.A., Srivastava, D., and Henkemeyer, M. (2004). Ephrin-B2 reverse signaling is required for axon pathfinding and cardiac valve formation but not early vascular development. Dev. Biol. *271*, 263–271.

Davy, A., and Soriano, P. (2005). Ephrin signaling in vivo: look both ways. Dev. Dyn. *232*, 1–10.

Davy, A., Aubin, J., and Soriano, P. (2004). Ephrin-B1 forward and reverse signaling are required during mouse development. Genes Dev. *18*, 572–583.

Ducy, P., Zhang, R., Geoffroy, V., Ridall, A.L., and Karsenty, G. (1997). Osf2/Cbfa1: a transcriptional activator of osteoblast differentiation. Cell *89*, 747–754.

Etienne-Manneville, S., and Hall, A. (2002). Rho GTPases in cell biology. Nature *420*, 629–635.

Franzoso, G., Carlson, L., Xing, L., Poljak, L., Shores, E.W., Brown, K.D., Leonardi, A., Tran, T., Boyce, B.F., and Siebenlist, U. (1997). Requirement for NF-κB in osteoclast and B-cell development. Genes Dev. *11*, 3482–3496.

Füller, T., Korff, T., Kilian, A., Dandekar, G., and Augustin, H.G. (2003). Forward EphB4 signaling in endothelial cells controls cellular repulsion and segregation from ephrinB2 positive cells. J. Cell Sci. *116*, 2461–2470.

Gale, N.W., and Yancopoulos, G.D. (1999). Growth factors acting via endothelial cell-specific receptor tyrosine kinases: VEGFs, angiopoietins, and ephrins in vascular development. Genes Dev. *13*, 1055–1066.

Gebbink, M.F., Kranenburg, O., Poland, M., van Horck, F.P., Houssa, B., and Moolenaar, W.H. (1997). Identification of a novel, putative Rho-specific GDP/GTP exchange factor and a RhoA-binding protein: control of neuronal morphology. J. Cell Biol. *137*, 1603–1613.

Gerety, S.S., and Anderson, D.J. (2002). Cardiovascular ephrinB2 function is essential for embryonic angiogenesis. Development *129*, 1397–1410.

Gerety, S.S., Wang, H.U., Chen, Z.F., and Anderson, D.J. (1999). Symmetrical mutant phenotypes of the receptor EphB4 and its specific transmembrane ligand ephrin-B2 in cardiovascular development. Mol. Cell *4*, 403–414.

Grigoriadis, A.E., Wang, Z.Q., Cecchini, M.G., Hofstetter, W., Felix, R., Fleisch, H.A., and Wagner, E.F. (1994). c-Fos: a key regulator of osteoclast-macrophage lineage determination and bone remodeling. Science *266*, 443–448.

Harmey, D., Stenbeck, G., Nobes, C.D., Lax, A.J., and Grigoriadis, A.E. (2004). Regulation of osteoblast differentiation by *Pasteurella multocida* toxin (PMT): a role for Rho GTPase in bone formation. J. Bone Miner. Res. *19*, 661–670.

Harris, W.H., and Heaney, R.P. (1969). Skeletal renewal and metabolic bone disease. N. Engl. J. Med. *280*, 253–259.

Hattner, R., Epker, B.N., and Frost, H.M. (1965). Suggested sequential mode of control of changes in cell behaviour in adult bone remodelling. Nature *206*, 489–490.

Hayden, J.M., Mohan, S., and Baylink, D.J. (1995). The insulin-like growth factor system and the coupling of formation to resorption. Bone *17*, 93S–98S.

Himanen, J.P., and Nikolov, D.B. (2003). Eph receptors and ephrins. Int. J. Biochem. Cell Biol. *35*, 130–134.

Ishida, N., Hayashi, K., Hoshijima, M., Ogawa, T., Koga, S., Miyatake, Y., Kumegawa, M., Kimura, T., and Takeya, T. (2002). Large scale gene expression analysis of osteoclastogenesis *in vitro* and elucidation of NFAT2 as a key regulator. J. Biol. Chem. *277*, 41147–41156.

Jaiswal, R.K., Jaiswal, N., Bruder, S.P., Mbalaviele, G., Marshak, D.R., and Pittenger, M.F. (2000). Adult human mesenchymal stem cell differentiation to the osteogenic or adipogenic lineage is regulated by mitogen-activated protein kinase. J. Biol. Chem. *275*, 9645–9652.

Kanzaki, S., Ito, M., Takada, Y., Ogawa, K., and Matsuo, K. (2006). Resorption of auditory ossicles and hearing loss in mice lacking osteoprotegerin. Bone *39*, 414–419.

Karsenty, G., and Wagner, E.F. (2002). Reaching a genetic and molecular understanding of skeletal development. Dev. Cell *2*, 389–406.

Komori, T., Yagi, H., Nomura, S., Yamaguchi, A., Sasaki, K., Deguchi, K., Shimizu, Y., Bronson, R.T., Gao, Y.H., Inada, M., et al. (1997). Targeted disruption of *Cbfa1* results in a complete lack of bone formation owing to maturational arrest of osteoblasts. Cell *89*, 755–764.

Kullander, K., and Klein, R. (2002). Mechanisms and functions of Eph and ephrin signalling. Nat. Rev. Mol. Cell Biol. *3*, 475–486.

Liu, W., Toyosawa, S., Furuichi, T., Kanatani, N., Yoshida, C., Liu, Y., Himeno, M., Narai, S., Yamaguchi, A., and Komori, T. (2001). Overexpression of Cbfa1 in osteoblasts inhibits osteoblast maturation and causes osteopenia with multiple fractures. J. Cell Biol. *155*, 157–166.

Martin, T.J. (2004). Does bone resorption inhibition affect the anabolic response to parathyroid hormone? Trends Endocrinol. Metab. *15*, 49–50.

Matsuo, K., Galson, D.L., Zhao, C., Peng, L., Laplace, C., Wang, K.Z., Bachler, M.A., Amano, H., Aburatani, H., Ishikawa, H., and Wagner, E.F. (2004). Nuclear factor of activated T-cells (NFAT) rescues osteoclastogenesis in precursors lacking c-Fos. J. Biol. Chem. *279*, 26475–26480.

McBeath, R., Pirone, D.M., Nelson, C.M., Bhadriraju, K., and Chen, C.S. (2004). Cell shape, cytoskeletal tension, and RhoA regulate stem cell lineage commitment. Dev. Cell *6*, 483–495.

Murai, K.K., and Pasquale, E.B. (2003). 'Eph'ective signaling: forward, reverse and crosstalk. J. Cell Sci. *116*, 2823–2832.

Myshkin, E., and Wang, B. (2003). Chemometrical classification of ephrin ligands and Eph kinases using GRID/CPCA approach. J. Chem. Inf. Comput. Sci. *43*, 1004–1010.

Nakashima, K., Zhou, X., Kunkel, G., Zhang, Z., Deng, J.M., Behringer, R.R., and de Crombrugghe, B. (2002). The novel zinc finger-containing transcription factor osterix is required for osteoblast differentiation and bone formation. Cell *108*, 17–29.

Nishiwaki, T., Yamaguchi, T., Zhao, C., Amno, H., Hankenson, K.D., Bornstein, P., Toyama, Y., and Matsuo, K. (2006). Reduced expression of thrombospondins and craniofacial dysmorphism in mice overexpressing Fra1. J. Bone Miner. Res. *21*, 596–604.

Noren, N.K., and Pasquale, E.B. (2004). Eph receptor-ephrin bidirectional signals that target Ras and Rho proteins. Cell. Signal. *16*, 655–666.

Palmer, A., and Klein, R. (2003). Multiple roles of ephrins in morphogenesis, neuronal networking, and brain function. Genes Dev. *17*, 1429–1450.

Parfitt, A.M. (1994). Osteonal and hemi-osteonal remodeling: the spatial and temporal framework for signal traffic in adult human bone. J. Cell. Biochem. *55*, 273–286.

Pasquale, E.B. (2005). Eph receptor signalling casts a wide net on cell behaviour. Nat. Rev. Mol. Cell Biol. *6*, 462–475.

Pfeilschifter, J., and Mundy, G.R. (1987). Modulation of type beta transforming growth factor activity in bone cultures by osteotropic hormones. Proc. Natl. Acad. Sci. USA *84*, 2024–2028.

Ray, N., Kuwahara, M., Takada, Y., Maruyama, K., Kawaguchi, T., Tsubone, H., Ishikawa, H., and Matsuo, K. (2006). c-Fos suppresses systemic inflammatory response to endotoxin. Int. Immunol. *18*, 671–677.

Sharfe, N., Freywald, A., Toro, A., Dadi, H., and Roifman, C. (2002). Ephrin stimulation modulates T cell chemotaxis. Eur. J. Immunol. *32*, 3745–3755.

Sheu, T.-J., Schwarz, E.M., Martinez, D.A., O'Keefe, R.J., Rosier, R.N., Zuscik, M.J., and Puzas, J.E. (2003). A phage display technique identifies a novel regulator of cell differentiation. J. Biol. Chem. *278*, 438–443.

Steinle, J.J., Meininger, C.J., Forough, R., Wu, G., Wu, M.H., and Granger, H.J. (2002). Eph B4 receptor signaling mediates endothelial cell migration and proliferation via the phosphatidylinositol 3-kinase pathway. J. Biol. Chem. *277*, 43830–43835.

Takayanagi, H., Kim, S., Koga, T., Nishina, H., Isshiki, M., Yoshida, H., Saiura, A., Isobe, M., Yokochi, T., Inoue, J., et al. (2002a). Induction and activation of the transcription factor NFATc1 (NFAT2) integrate RANKL signaling in terminal differentiation of osteoclasts. Dev. Cell *3*, 889–901.

Takayanagi, H., Kim, S., Matsuo, K., Suzuki, H., Suzuki, T., Sato, K., Yokochi, T., Oda, H., Nakamura, K., Ida, N., et al. (2002b). RANKL maintains bone homeostasis through c-Fos-dependent induction of interferon-β. Nature *416*, 744–749.

Teitelbaum, S.L., and Ross, F.P. (2003). Genetic regulation of osteoclast development and function. Nat. Rev. Genet. *4*, 638–649.

Wang, F.-S., Wang, C.-J., Sheen-Chen, S.-M., Kuo, Y.-R., Chen, R.-F., and Yang, K.D. (2002). Superoxide mediates shock wave induction of ERK-dependent osteogenic transcription factor (CBFA1) and mesenchymal cell differentiation toward osteoprogenitors. J. Biol. Chem. *277*, 10931–10937.

Wang, H.U., Chen, Z.F., and Anderson, D.J. (1998). Molecular distinction and angiogenic interaction between embryonic arteries and veins revealed by ephrin-B2 and its receptor Eph-B4. Cell *93*, 741–753.

Wang, Z.Q., Ovitt, C., Grigoriadis, A.E., Möhle-Steinlein, U., Rüther, U., and Wagner, E.F. (1992). Bone and haematopoietic defects in mice lacking c-*fos*. Nature *360*, 741–744.

Wang, Z., Cohen, K., Shao, Y., Mole, P., Dombkowski, D., and Scadden, D.T. (2004). Ephrin receptor, EphB4, regulates ES cell differentiation of primitive mammalian hemangioblasts, blood, cardiomyocytes, and blood vessels. Blood *103*, 100–109.

Xiao, G., Jiang, D., Thomas, P., Benson, M.D., Guan, K., Karsenty, G., and Franceschi, R.T. (2000). MAPK pathways activate and phosphorylate the osteoblast-specific transcription factor, Cbfa1. J. Biol. Chem. *275*, 4453–4459.

Yu, G., Luo, H., Wu, Y., and Wu, J. (2003). Ephrin B2 induces T cell costimulation. J. Immunol. *171*, 106–114.